Main dipoles of the CNAO accelerator: some general features and systematic effects associated with fluxmeter-based magnetic measurements

Maud Baylac

Main dipoles of the CNAO accelerator: some general features and systematic effects associated with fluxmeter-based magnetic measurements

Maud BAYLAC
Note interne LPSC 07-71

This report presents some general characteristics of the main synchrotron dipole magnets designed for the CNAO project [1]. It gives some estimates of field integrals and magnetic field flux using the TOSCA field maps. Then it aims to evaluate some systematic effects associated to the magnetic measurements planned with the fluxmeter, especially designed to characterize the CNAO dipoles [2]. All of what follows was performed at maximum magnetic field (1.5 T) without magnet shimming.

In this report, we will only consider the half-dipole (z>0) which corresponds to the available field maps. We will abusively refer to the quantities we will calculate using these fields maps as field integrals and field fluxes, whereas they represent "half-integrals" or "half-fluxes". The dipole is considered perfectly symmetric around the central plane (z=0) so that all quantities quoted thereafter must be multiplied by 2. The dipole is also considered to be symmetric around the median plane (y=0), such that sole field maps with y>0 are generated.

1. Definition and notations

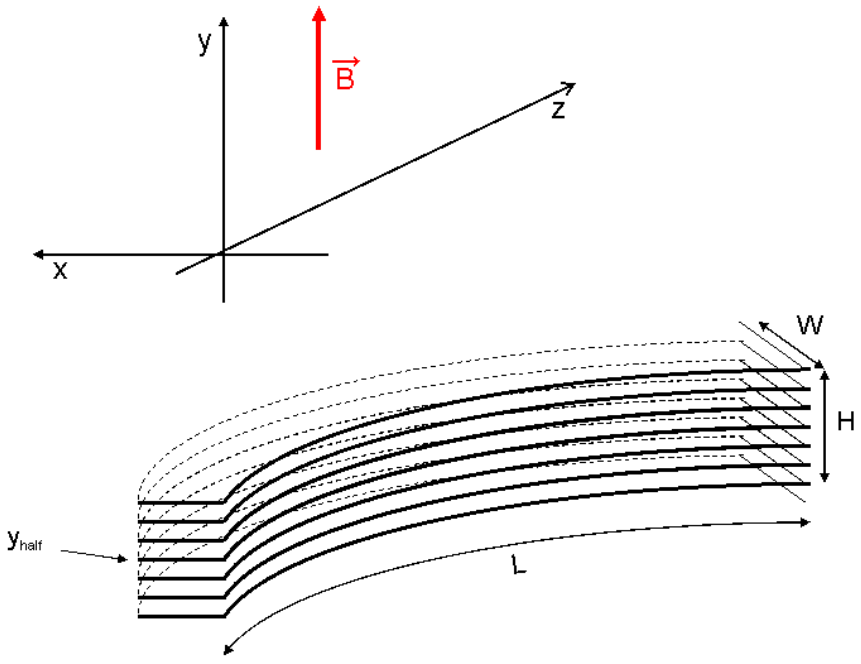

Figure 1: schematics of the fluxmeter model.

The fluxmeter is modeled as a series of horizontal curved coils. Each coil consists of N spires of identical length L and width W. The total height of each coil is H. We note the surface of each spire j, S_j where S_j=S. The magnetic field is at first considered purely vertical $\vec{B} = B_y \vec{y}$. A schematic view is given in figure 1.

The field integral is calculated in each of the N horizontal planes and for trajectories separated by δ_x = 1 mm across the width of the good field region (-60≤ x ≤+60 mm). The theoretical field maps were generated [3] using the longitudinal step δ_z = 2.5 mm. The distance dl along the trajectory between 2 adjacent data points on a trajectory of the field map labeled by the indices iz and iz+1 (see fig. 2) is approximated to be:

$$dl \approx \sqrt{(x_{iz+1} - x_{iz})^2 + (z_{iz+1} - z_{iz})^2} \tag{1}$$

The elemental surface *ds* span between 4 adjacent data points on the mesh (fig. 2) is:

$$\begin{aligned} ds &\approx dx \times dl \\ ds &\approx (x_{ix+1,iz} - x_{ix,iz}) \times (z_{ix,iz+1} - z_{ix,iz}) \end{aligned} \tag{2}$$

The field over the distance dl is considered constant and equal to the average of the field at the 2 end points. The field integral along each trajectory iz at a vertical coordinate y and a transverse coordinate defined in the center plane of the magnet (z=0) x^{center}, is thus calculated as:

$$I(x_{ix}^{center}, y) = \frac{1}{2}\sum_{iz}\left[B(x_{ix,iz}, y, z_{ix,iz}) + B(x_{ix,iz+1}, y, z_{ix,iz+1})\right]\sqrt{(x_{iz+1} - x_{iz})^2 + (z_{iz+1} - z_{iz})^2} \tag{3}$$

The magnetic flux $\Phi(j)$ through each spire *j* is:

$$\Phi(j) = \sum_{ix,iz} d\Phi_{ix,iz}$$

$$\begin{aligned} \Phi(j) = \frac{1}{4} \times \sum_{ix,iz}\Big[&B(x_{ix,iz}, y_j, z_{ix,iz}) + B(x_{ix+1,iz}, y_j, z_{ix+1,iz}) + B(x_{ix,iz+1}, y_j, z_{ix,iz+1}) + B(x_{ix+1,iz+1}, y_j, z_{ix+1,iz+1})\Big] \\ &\times (x_{ix+1,iz} - x_{ix,iz}) \times (z_{ix,iz+1} - z_{ix,iz}) \end{aligned} \tag{4}$$

where y_j represents the vertical position y in the plane of the spire *j*.

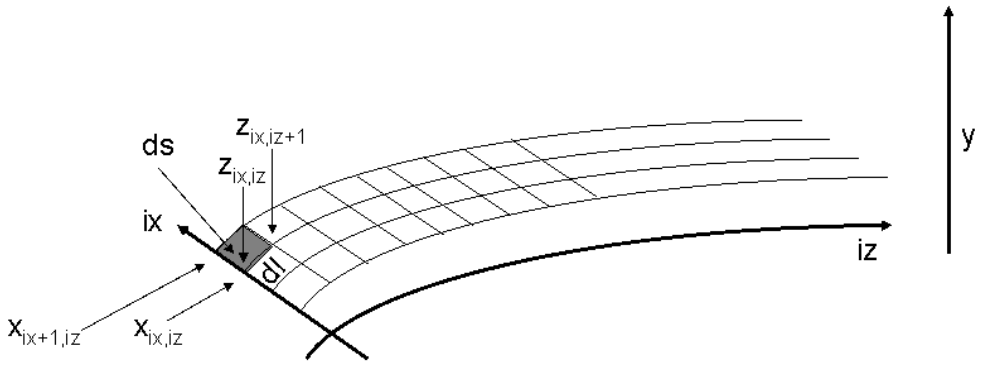

Figure 2: schematics of the notation used for the magnetic field flux calculation. Each data point of the mesh for each vertical plane (y) is labelled with an index iz running along a given trajectory and an index ix corresponding to the transverse location of the trajectory.

2. Magnetic field

Figure 3 displays the vertical component of the magnetic field B_y as a function of the longitudinal position along the magnet z and its first derivative along z, dB_y/dz determined along the z axis (x=y=0). The longitudinal variation of the magnetic field is maximum a few cm before the edge where it reaches 20%.

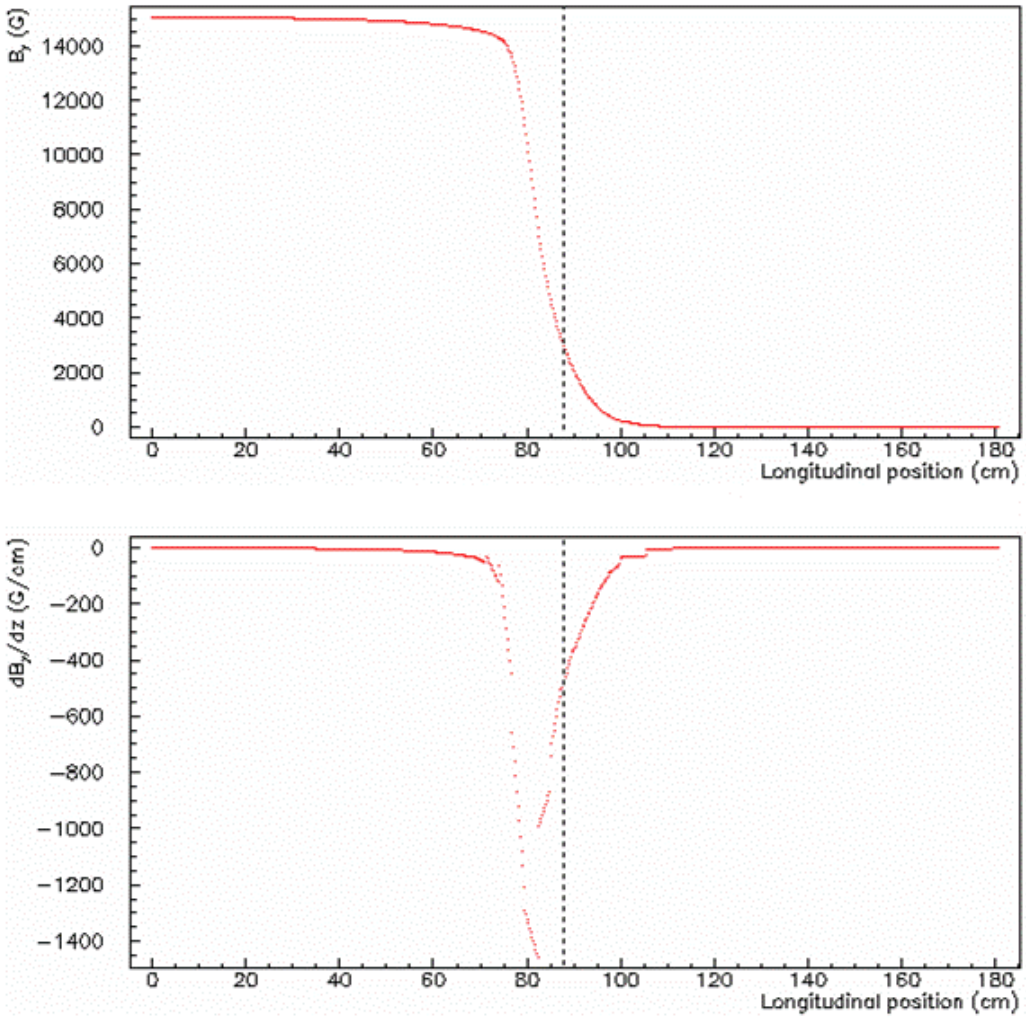

Figure 3: Vertical component of the magnetic field B_y (top) and its first derivative dB_y/dz (bottom) as a function of the longitudinal position z along the central trajectory along the z axis (x=y=0). The dashed line represents the edge of the magnet.

3. Check of the parabolic behavior of the magnetic field with the vertical position

In order to get a rough model of the vertical component of the magnetic field, one can try and express the field in a vertical plane (z=constant) as a parabolic function of the vertical position:

$$B_y(x,y,z) = \beta(x,z) + B(x,z)\, y^2$$
$$= \beta(x,z) + \alpha\, y^2 \qquad (5)$$

By fitting the values of the field $B_y(x,y,z)$ from the available field maps in different vertical planes (fig. 4), one can determine regions (as a function of the longitudinal coordinate z) where the parabolic approximation is valid:

- $0 \leq |z| \leq 77$ cm: $\alpha > 0$
- $82 \leq |z| \leq 131$ cm: $\alpha < 0$
- $143 \leq |z| \leq 180$ cm: $\alpha > 0$

It is therefore valid in most of the volume that the dipole field can be approximated by a parabolic function of the vertical position in the good field region.

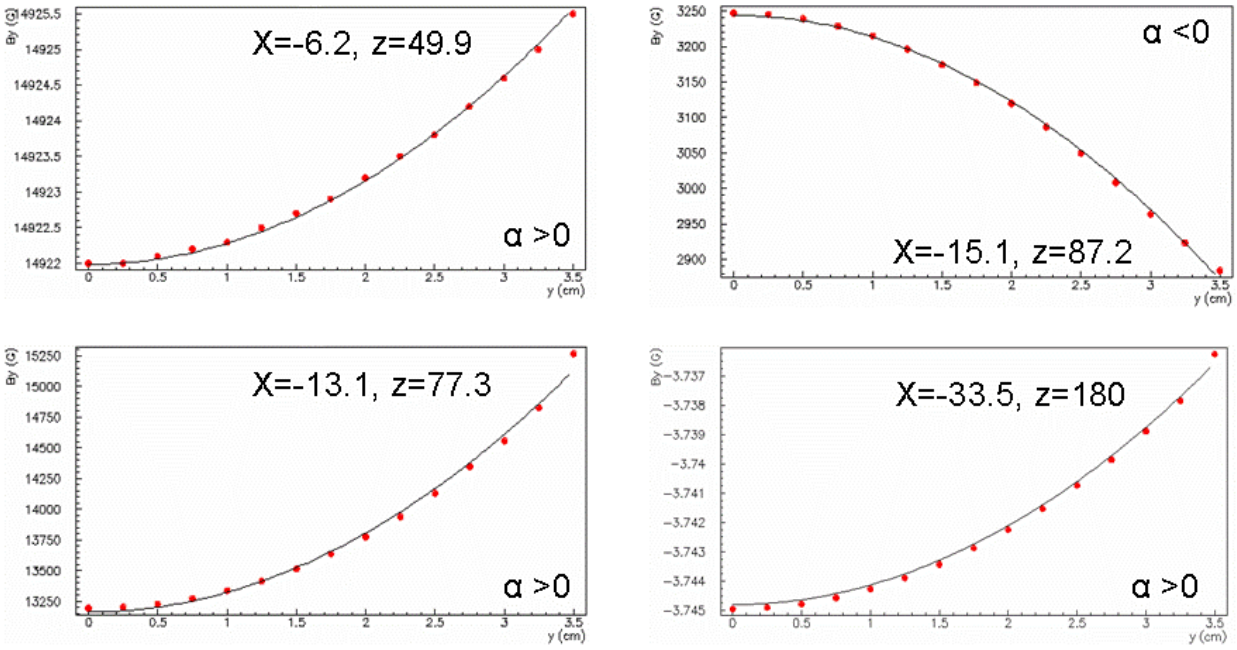

Figure 4: Magnetic field as a function of the vertical coordinate y for given x and z coordinates. Superposed to the data is a parabolic fit (see eq. 5). The parabolic coefficient α is positive except in a ~5 cm long region around the edge of the magnet.

4. Field integral

We first calculate the integral of the magnetic field along each trajectory (ie: along z), $\int B_y(x,y,z)dz$, as a function of the transverse coordinate x and for different vertical planes (figure 5). The field integral is calculated in 9 different planes, equally spaced around the plane of reference (Y=0 or Y=+29 mm) and separated by δ_y = 0.5 mm. For example, the field integral is calculated along trajectories for y=27, 27.5, 28, 28.5,…., 30.5, 31 mm. Figure 5 displays the 9 individual integrals, as a function of the transverse position x measured in the center plane of the magnet (z=0) x^{center}. One can see that the field integral varies with x across the good field region (maximum span ~0.2%). The maximum field integral does not correspond to the center of magnet (x=0) but to a positive value of x, *ie*: left of the central trajectory. Around the median plane, the field integral is nearly constant across a 4 mm height. But around the Y=+29 mm plane, the field integral varies with the vertical position.

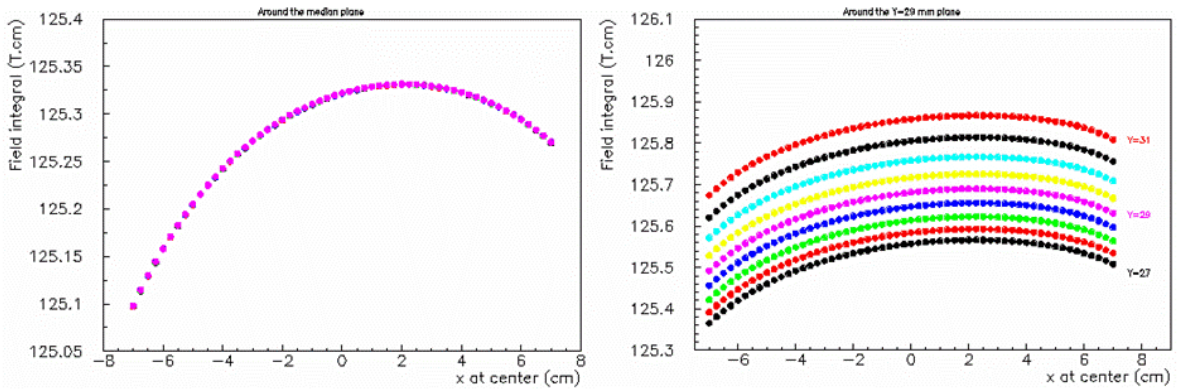

Figure 5: Integral of the magnetic field along a trajectory as a function of the transverse coordinate x. The 9 different curves on each plot correspond to different vertical planes equally spaced by 0.5 mm above and below the median plane (left) and the Y=+29 mm plane (right). All 9 curves around the median plane are indistinguishable.

To get a first idea of the systematic effect due to this variation across the height of the measuring coil, we compute for a given x the 2 following estimates:

- the sum of all 9 field integrals at different y values;
- 9 times the field integral determined for the central value of y (Y=0 or Y=+29mm).

Figure 6 displays the relative discrepancy between the 2 estimates. We can see that the discrepancy is negligible around the median plane but becomes on the same order of magnitude than the required magnet uniformity around Y=+29 mm (~2.10^{-4}). The sum of all 9 individual field integrals is always larger than 9 times the central field integral.

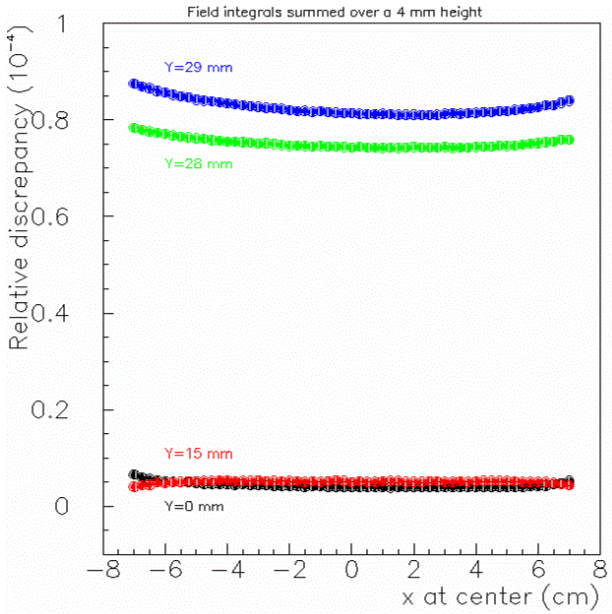

Figure 6: Relative discrepancy between the sum of individual field integrals at different vertical positions and an average using the field integral at the central vertical position, as a function of the transverse position x in the magnet center (z=0). The different curves correspond to the discrepancy calculated around different vertical positions: Y=0, Y=+15, Y=28 and Y=+29 mm.

5. Check of parabolic behavior of the field integral with vertical position

Figure 7 (left) shows the field integrals I(y) calculated along a trajectory at x=0 for different vertical positions y. Superimposed is a fit following $I(y) = \alpha y^2 + \beta$. One can see that the field integral is well described by a parabolic behavior in a region around the median plane (y<20 mm), but this form fails to reproduce the field map data as we get closer to the magnet poles. Indeed, we can see that the field integral grows exponentially with the vertical position when approaching the magnet poles. Figure 7 (right) displays the relative discrepancy between the field integral for a given vertical position y (for x=0) and the field integral in the median plane (x=y=0) away from the median (y>10 mm). One can see that the discrepancy is well described by an exponential function of y close to the poles (y>26 mm).

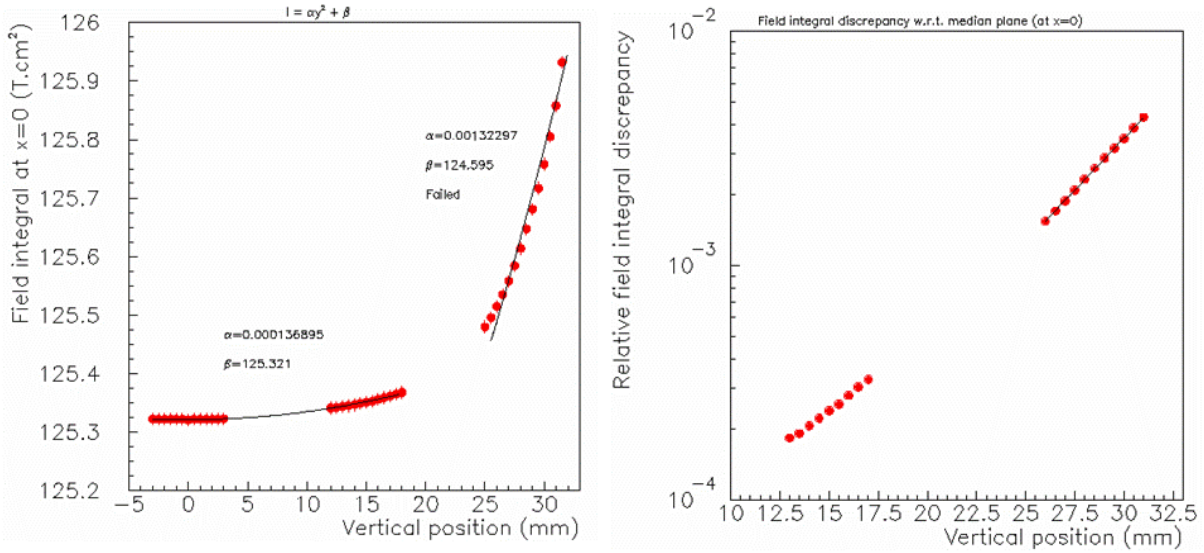

Figure 7: left: Field integrals determined for x=0 as a function of the vertical position y. Superimposed is a fit assuming a parabolic behavior; right: relative discrepancy between the field integral at a given y and at y=0 (log scale). Superimposed is a fit assuming an exponential behavior.

6. Magnetic field flux

The magnetic flux is calculated in 9 different spires, equally spaced around the plane of reference (Y=0 or Y=+29 mm) and separated by δ_y = 0.5 mm. Each magnetic flux is determined over a 1 mm wide spire and along the length of the spire. Figure 8 displays the 9 individual fluxes as a function of the transverse position x measured in the center plane of the magnet. We can already see that the discrepancy between fluxes at different vertical position is very small around the median plane but becomes measurable as we get closer to the magnet poles.

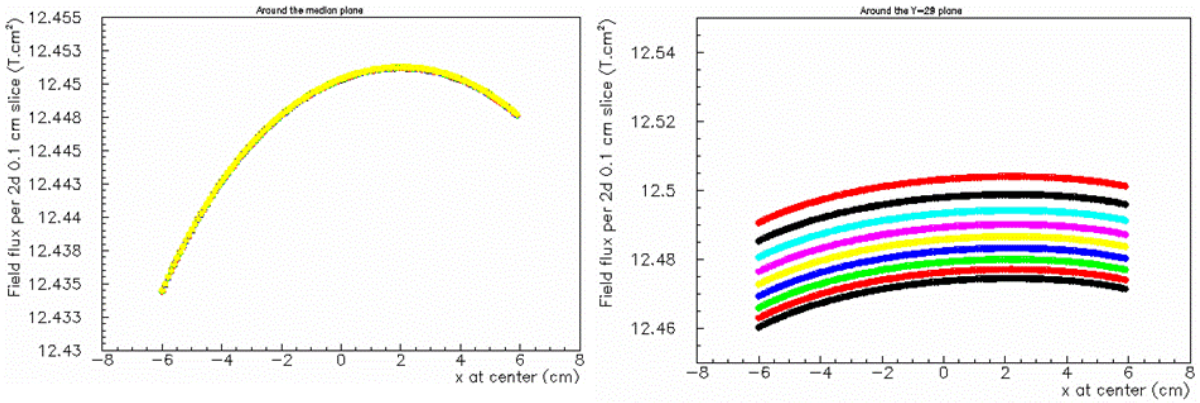

Figure 8: magnetic flux determined in a 1 mm wide spire as a function of the transverse position x^{center} for 9 vertical planes equally spaced by 0.5 mm above and below the median plane (left) and the plane Y=+29 mm (right). Each curve represents a vertical plane, the lowest flux corresponding to the lowest value of y. All 9 curves around the median plane are indistinguishable.

7. Flux of the magnetic field through the measuring coil: effect of the coil dimensions

To mimic the fluxmeter designed for the CNAO dipole magnetic measurements, we calculate the flux of the magnetic field through an 8 mm width, corresponding to the width of the measuring spires (fig. 9, left). Then we sum (or average, depending on the method used for the calculation, as described below) the fluxes determined at given vertical positions over a 4 mm height, corresponding to the height of the measuring coil (fig. 9, right).

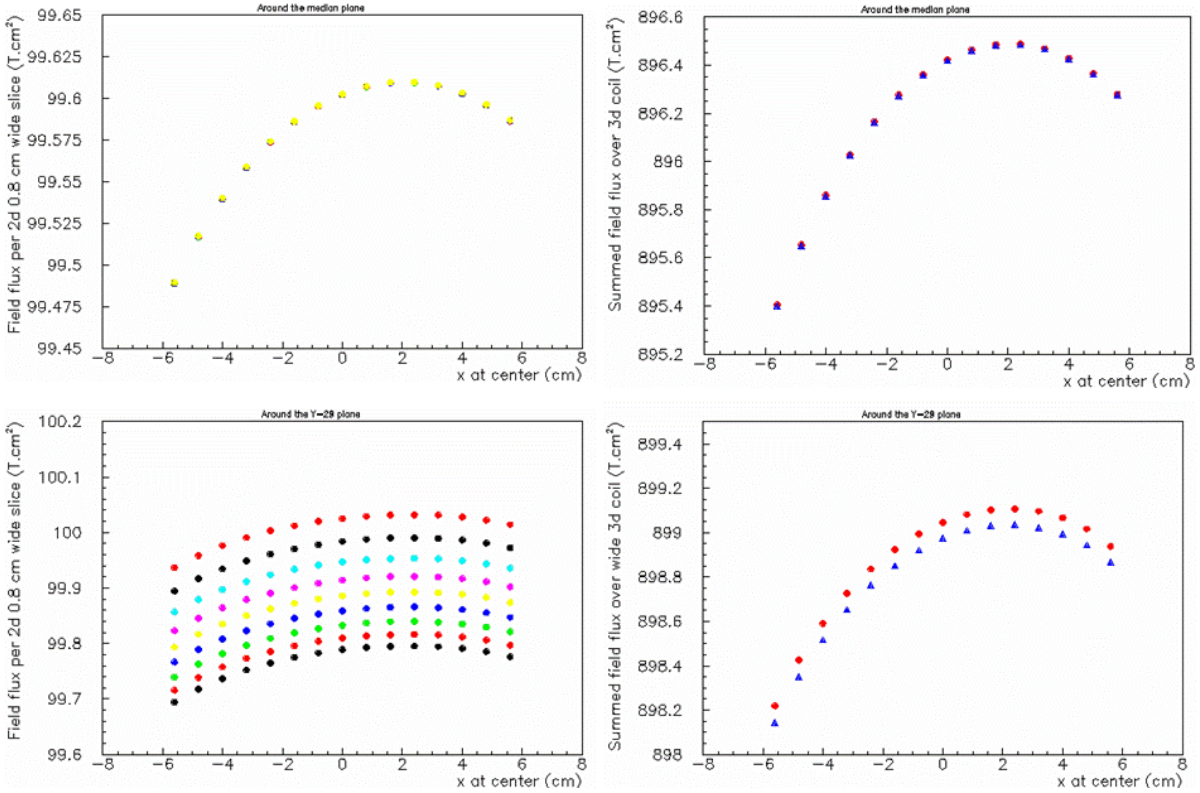

Figure 9: Simulation of the flux of the magnetic field through a single (2d) spire of the CNAO fluxmeter (left) and through a (3d) coil consisting of 9 individual spires seating on top on each other (right) as a function of the transverse position at the magnet center. On the right plot,

dots (stars) correspond to the flux through the coil determined with method 1 (2). Calculations were done around the median plane (top) and around the Y=+29 mm plane (bottom).

In order to estimate the systematic error of the fluxmeter measurement induced by the variations of the field across the height of the coil, we will compare 2 methods to determine the magnetic flux integrated over the height of the coil:

- Method 1: the magnetic flux is calculated as the sum of all individual fluxes at different vertical positions y_i determined using the value of the field at that position $B(y_i)$;
- Method 2: the magnetic flux is calculated assuming that the magnetic field is constant across the height of the coil and equal to the value of the field at mid-height of the coil $B(y_i) = B(y_{half})$,

the first method being the most similar to the actual measurement.

Method 1:
The total flux through each coil consisting of N spires is:

$$\Phi_1 = \sum_{j=1}^{N} \Phi(j)$$

$$= \frac{1}{4} \sum_{j=1}^{N} \sum_{ix,iz} [B(x_{ix,iz},y_j,z_{ix,iz})+B(x_{ix+1,iz},y_j,z_{ix+1,iz})+B(x_{ix,iz+1},y_j,z_{ix,iz+1})+B(x_{ix+1,iz+1},y_j,z_{ix+1,iz+1})]$$

$$. (x_{ix+1,iz} - x_{ix,iz}) . (z_{ix,iz+1} - z_{ix,iz}) \qquad (6)$$

Method 2:
The total flux through each coil consisting of N spires is:

$$\Phi_2 = \sum_{j=1}^{N} \Phi(j)$$

$$= \frac{1}{4} \sum_{j=1}^{N} (x_{ix+1,iz} - x_{ix,iz}) . (z_{ix,iz+1} - z_{ix,iz}) .$$

$$\sum_{ix,iz} [B(x_{ix,iz},y_{half},z_{ix,iz})+B(x_{ix+1,iz},y_{half},z_{ix+1,iz})+B(x_{ix,iz+1},y_{half},z_{ix,iz+1})+B(x_{ix+1,iz+1},y_{half},z_{ix+1,iz+1})]$$

$$= \frac{1}{4} .N. (x_{ix+1,iz} - x_{ix,iz}) . (z_{ix,iz+1} - z_{ix,iz}) .$$

$$\sum_{ix,iz} [B(x_{ix,iz},y_{half},z_{ix,iz})+B(x_{ix+1,iz},y_{half},z_{ix+1,iz})+B(x_{ix,iz+1},y_{half},z_{ix,iz+1})+B(x_{ix+1,iz+1},y_{half},z_{ix+1,iz+1})] \qquad (7)$$

8. Discussion & conclusion

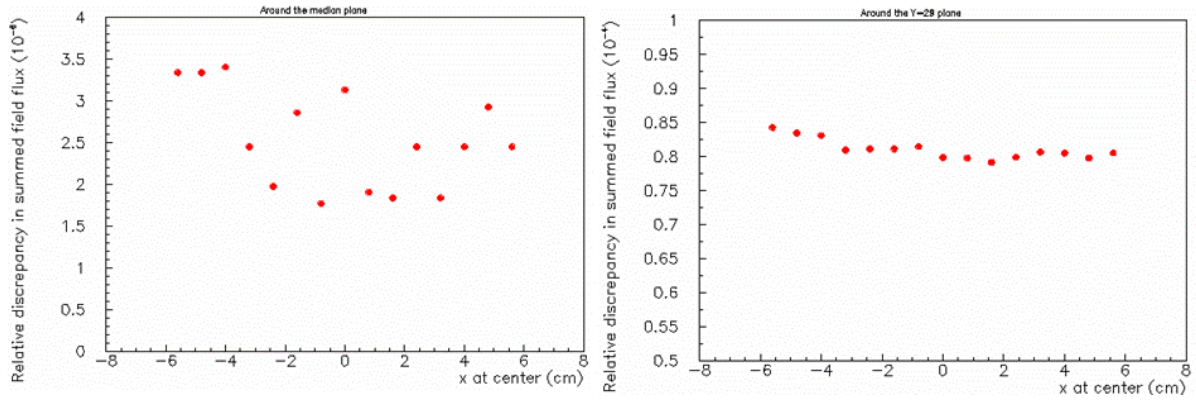

Figure 10: Relative discrepancy between the magnetic field fluxes calculated using a sum over the different spires (method 1) and using a single field value for all spires (method 2) around the median plane (left) and around the Y=+29 mm plane (right).

Looking at figures 6 and 10, one can see that the discrepancy in the field flux in the simulated measuring coil is similar to the discrepancy in the field integral. Comparing the field integral in figure 5 and the field flux in the simulated measuring coil shown in figure 9, we find that the width of the coil (in the horizontal plane) has hardly any effect and that the variations in field flux are mainly induced by the height of the coil, although both dimensions are comparable (8 mm width and 4 mm height). To understand these 2 different behaviours, we look at the variation of the magnetic field (and therefore of field flux) with each transverse coordinate. Figure 11 displays the magnetic field as a function of the transverse coordinate x and its first derivative with respect to x. The variation of magnetic field with x is negligible in the magnet center (along the x axis) where $|\frac{dB_y}{dx}| < 0.5$ G/cm, but becomes larger in the fringe fields where $\frac{dB_y}{dx}$ reaches ~40 G/cm. The slope determined at the magnet end yields an estimate of the field variation across the width of the coil, $\Delta B(width)$:

$$\Delta B(width) = \frac{dB_y}{dx}\Delta x \approx 40 \times 0.8 \approx 30 \text{ G}.$$

The relative variation of the field at this location is thus:

$$\frac{\Delta B(width)}{B(width)} \approx \frac{30}{7700} \approx 4.10^{-3}$$

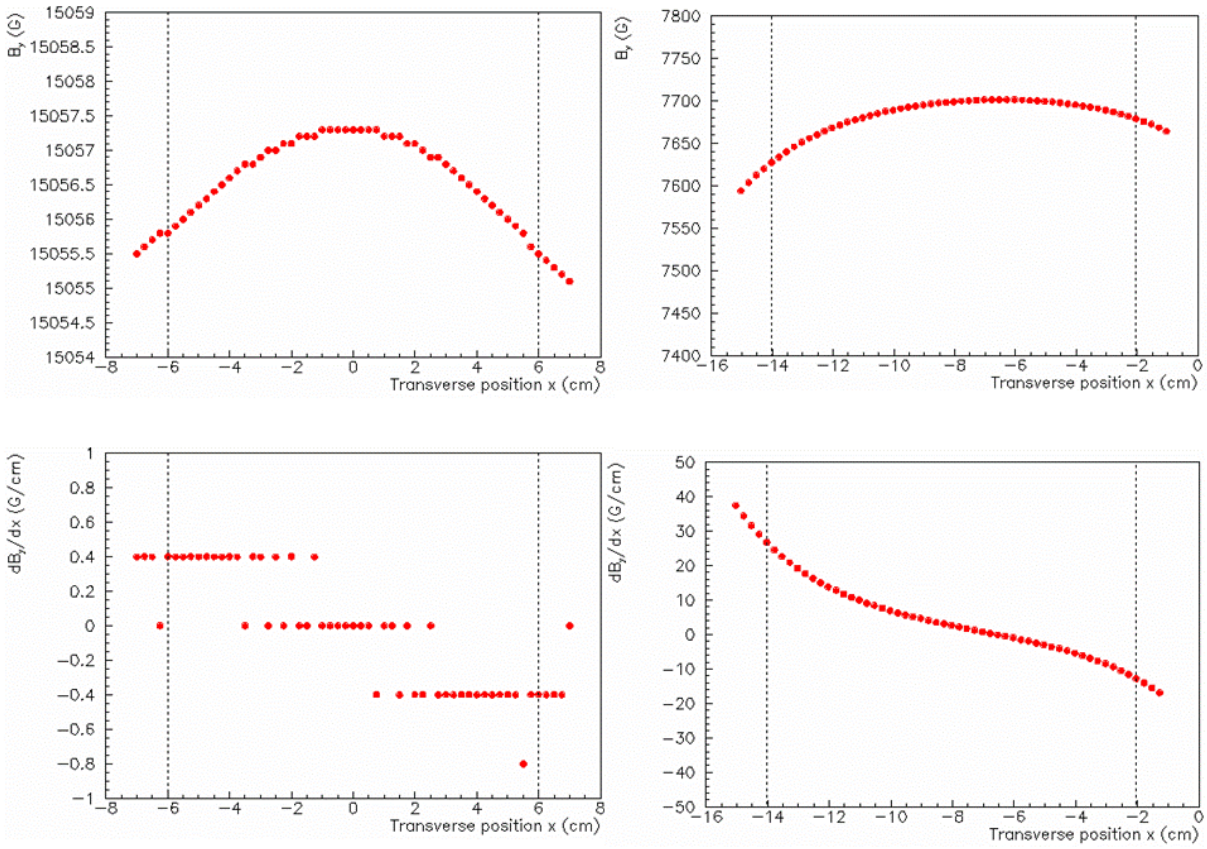

Figure 11: Vertical component of the magnetic field B_y (top) and its first derivative dB_y/dx (bottom) as a function of the vertical position x along the x axis (y=z=0) of the magnet (left) and at the intersection of the median plane and the plane of the magnet edge (y=0, z=82 cm). The dashed line represents the good field region. The discrete aspect of the lower left plot is an artifact of the calculus resolution as dB_y/dx is very small at the magnet center.

In the same way, we can estimate the effect of the height of the measuring coil. The sensitivity of the field to y variation, negligible in the magnet center, becomes significant in the fringe field, where $\frac{dB_y}{dx} \approx 1000\,\mathrm{G/cm}$ around Y=+29 mm (fig. 12). The field variation across the height of the coil, $\Delta B(height)$, is thus:

$$\Delta B(height) = \frac{dB_y}{dy}\Delta y \approx 800 \times 0.4 \approx 300\,\mathrm{G},$$

and its relative contribution becomes:

$$\frac{\Delta B(width)}{B(width)} \approx \frac{300}{7700} \approx 4.10^{-2}$$

The variation of the magnetic field, and therefore of the field flux, across the height of the coil, is thus 10 times larger than its variation across the width in the fringe field. Moreover, unlike $\frac{dB_y}{dx}$ which exhibits a smooth behavior across x, the sensitivity $\frac{dB_y}{dy}$ varies dramatically around the limits of the good field region (y > 25 mm). The accuracy of the fluxmeter

measurement in this region is then questionable as we will become very sensitive to coil height as well as the vertical coil positioning and alignment.

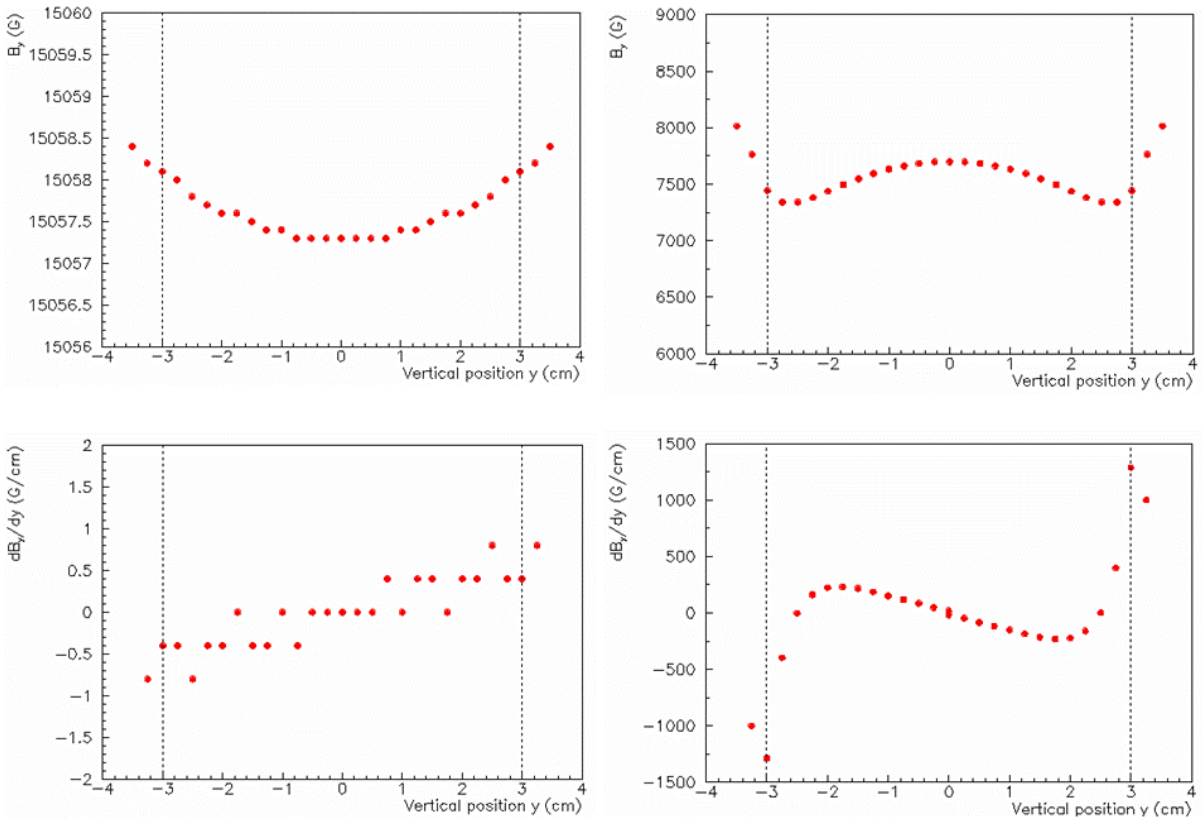

Figure 12: Vertical component of the magnetic field B_y (top) and its first derivative dB_y/dy (bottom) as a function of the vertical position y along the y axis (x=z=0) of the magnet (left) and at the intersection of the median plane and the plane of the magnet edge (x=-8 cm, z=82 cm). The dashed line represents the good field region. The discrete aspect of the lower left plot is an artifact of the calculus resolution as dB_y/dy is very small at the magnet center.

The present study proved the validity of the fluxmeter measurement in the median plane of the CNAO dipoles. All estimations were done using the field maps generated before the magnet shimming. It is was found that it is accurate to equal the flux of the magnetic field through the measuring coil (8 mm wide and 4 mm high) with the flux in the median plane (Y=0 mm). Measurements outside of the median plane are found to be less straightforward as they are more sensitive to the dimensions of the measuring coil, this effect being more pronounced as we approach the magnet poles. In particular, when measuring the flux of the magnetic field around the highest plane of the foreseen measurements (Y=+29 mm) [2], the relative difference between the measurement with the simulated coil as the field varies across the coil's height (method 1) and a local estimation in the central plane of the coil is not negligible compared to the required dipole uniformity (2.10^{-4}). We therefore recommend that the accuracy of measurements in planes at the edges of the good field region (y > 25 mm) be considered with caution.

REFERENCES

1. Technical note CNA-TNDP-005WXX-00288, *The CNAO main ring dipole electromagnetic design report*, S. La Bella *et al*, Dec. 17, 2003.
2. *Detailed program of the magnetic measurements for the CNAO prototype dipole*, D. Cornuet, May 12, 2005, CERN-Tech-Note AT-MTM-RM-2005-36, EDMS 590342.
3. Many thanks to Cristiana PRIANO.